Geophysical Research Letters

RESEARCH LETTER
10.1029/2021GL094004

Key Points:

- The atmospheric cloud radiative effect (ACRE) depends on the column relative humidity (CRH) in a way similar to precipitation
- The CRH skillfully estimates ACRE on annual, monthly, and daily time scales in the tropics
- ACRE-cloud feedback suggested to explain the CRH-precipitation relationship by facilitating a shift from convective to stratiform rainfall

Supporting Information:

Supporting Information may be found in the online version of this article.

Correspondence to:
M. R. Needham,
m.needham@colostate.edu

Citation:
Needham, M. R., & Randall, D. A. (2021). Linking atmospheric cloud radiative effects and tropical precipitation. *Geophysical Research Letters*, *48*, e2021GL094004. https://doi.org/10.1029/2021GL094004

Received 11 MAR 2021
Accepted 23 JUN 2021

Linking Atmospheric Cloud Radiative Effects and Tropical Precipitation

Michael R. Needham[1] and **David A. Randall**[1]

[1]Department of Atmospheric Science, Colorado State University, Fort Collins, CO, USA

Abstract Studies in recent decades have demonstrated a robust relationship between tropical precipitation and column relative humidity (CRH). The present study identifies a similar relationship between CRH and the atmospheric cloud radiative effect (ACRE) calculated from satellite observations. Like precipitation, the ACRE begins to increase rapidly when CRH exceeds a critical value near 70%. We show that the ACRE can be estimated from CRH, similar to the way that CRH has been used to estimate precipitation. Our method reproduces the annual mean spatial structure of the ACRE in the tropics, and skillfully estimates the mean ACRE on monthly and daily time scales in six regions of the tropics. We propose that the exponential dependence of precipitation on CRH may be partially explained by cloud-longwave feedbacks, which facilitate a shift from convective to stratiform conditions.

Plain Language Summary The tropical precipitation rate can be estimated using a quantity called the column relative humidity (CRH), which quantifies how close the atmosphere is to becoming saturated with water. We show that the CRH can also be used to estimate the local radiative heating of the atmosphere due to clouds. The simple method used in this study can reproduce the average cloud radiative heating of the tropical atmosphere, and can be used to estimate the monthly average and daily average heating in six different tropical regions. We suggest that the relationship between precipitation and CRH may be related to cloud-radiative heating, which promotes precipitation in large-scale systems.

1. Introduction

The effects of clouds on the Earth's radiation balance can be quantified using the cloud radiative effect (CRE), defined as the difference between full-sky and clear-sky radiative fluxes (Ramanathan, 1987). The CRE manifests at the top of the atmosphere, where clouds increase the reflection of solar radiation while simultaneously enhancing greenhouse warming; at the surface, where cloud shading prevents solar absorption while emitting infrared radiation downwards; and in the atmosphere itself, where clouds warm or cool locally by absorbing or emitting radiation. A large body of work has investigated the impact of this atmospheric cloud radiative effect (ACRE) on the Earth's global circulation patterns (Li et al., 2015; Randall et al., 1989; Sherwood et al., 1994; Slingo & Slingo, 1988; Stevens et al., 2012; Voigt & Albern, 2019). For example, the ACRE has been found to widen the subsiding branches of the Hadley cells and narrow the Intertropical Convergence Zone (ITCZ) in idealized numerical simulations (Albern et al., 2018; Dixit et al., 2018; Harrop & Hartmann, 2016; Popp & Silvers, 2017; Voigt et al., 2021). Voigt et al. (2021) recently reviewed our current understanding of the interactions between clouds, radiation, and atmospheric circulations, with a particular emphasis on the ACRE.

The longwave ACRE has been identified as an important feedback mechanism in the context of the persistence of convective self-aggregation, the initial development of tropical cyclones, and the Madden-Julian Oscillation (Arnold & Randall, 2015; Benedict et al., 2020; Bretherton et al., 2005; Chikira, 2014; Emanuel, 2019; Khairoutdinov & Emanuel, 2018; Medeiros et al., 2021; Ruppert et al., 2020; Wing et al., 2017; Wolding et al., 2016). The longwave ACRE can be a strong localized atmospheric heating that induces a thermally direct circulation connecting humid and dry regions. Such a circulation can transport moisture against the gradient, into humid regions, which favors increased precipitation and cloudiness. This type of cloud-longwave feedback has been discussed in detail by Needham and Randall (2021) as companion to this study.

Recent observational and modeling studies have shown a strong link between atmospheric humidity and tropical precipitation (Ahmed & Schumacher, 2015; Bretherton et al., 2004; Inoue & Back, 2015; Powell, 2019; Masunaga & L'Ecuyer, 2014; Raymond, 2000; Raymond & Zeng, 2005; Raymond et al., 2009; Rushley et al., 2018; Wolding et al., 2020; Zeng, 1999). Bretherton et al. (2004) showed that tropical precipitation can be modeled as an exponential function of column relative humidity (CRH, defined as the ratio between the water vapor path and saturation water vapor path), and this relationship has been used in many applications including theoretical studies of the MJO (see Rushley et al., 2018, and references therein). More recently, Ahmed and Schumacher (2015) used observations from the DYNAMO field campaign (Yoneyama et al., 2013) and satellite estimates of precipitation to show that the rapid increase of precipitation in humid regions is due to stratiform rather than convective rainfall. Furthermore, they found that the area covered by stratiform precipitation accounts for much of the nonlinearity in the precipitation-humidity relationship, while the area covered by convective precipitation is only a weakly nonlinear function of the CRH.

In this study, we suggest a link between longwave-cloud feedbacks and the observed relationship between tropical precipitation and CRH. Section 2 describes the data. In Section 3, the ACRE is shown to be a strong function of the CRH, while Section 4 demonstrates that CRH may be used to estimate the tropical ACRE on annual mean, monthly, and daily time scales. Conclusions are discussed in Section 5.

2. Data and Methods

Top of atmosphere and surface fluxes of longwave and shortwave radiation come from the CERES SYN1deg Ed4a product (Doelling et al., 2013, hereafter CERES). CERES data were downloaded on a 1° × 1° grid. Daily mean radiative fluxes were used to calculate the CRE as the difference between full-sky and clear-sky fluxes. The CRE was calculated at the top of the atmosphere and at the surface, and the ACRE was calculated as the difference between the two.

Reanalysis fields of temperature and specific humidity were downloaded from ERA5 (Hersbach et al., 2018, 2020) at a temporal resolution of 6 h on the native 0.25° × 0.25° grid. The CRH was calculated as follows:

$$\mathrm{CRH} = \frac{\int_{p_t}^{p_s} q\,dp}{\int_{p_t}^{p_s} q^*\,(T)\,dp}, \tag{1}$$

where q^* is the saturation vapor pressure. The ERA5 data were averaged to daily means and to the coarser 1° × 1° CERES grid.

Both data sources span the same 19-years period from January 1, 2001 to December 31, 2019. Analysis was restricted to the tropical belt ranging from 30°S to 30°N. The analysis was repeated for six subset regions which represent the Indo-Pacific warm pool, Pacific ITCZ, south Pacific convergence zone (hereafter SPCZ), Pacific cold tongue, Atlantic ITCZ, and Atlantic cold tongue.

In addition, we utilize precipitation rates from the TRMM Multisatellite Precipitation Analysis (3B42 product, Huffman et al., 2016) to show climatology and to reproduce the exponential relationship between CRH and precipitation.

3. ACRE Binned by CRH

The tropical band ranging from 30°S to 30°N is characterized by wide distributions of precipitation and humidity (Figures 1a and 1b). This includes regions of warm SSTs with enhanced convection and regions of cool SSTs with suppressed convection. Land surface covers ~25% of this belt, which introduces additional complexity.

We now perform a binning analysis, following the method used in previous studies. The area-weighted average TRMM precipitation rate was found for each CRH bin of width 2% ranging from 0% to 100%. The

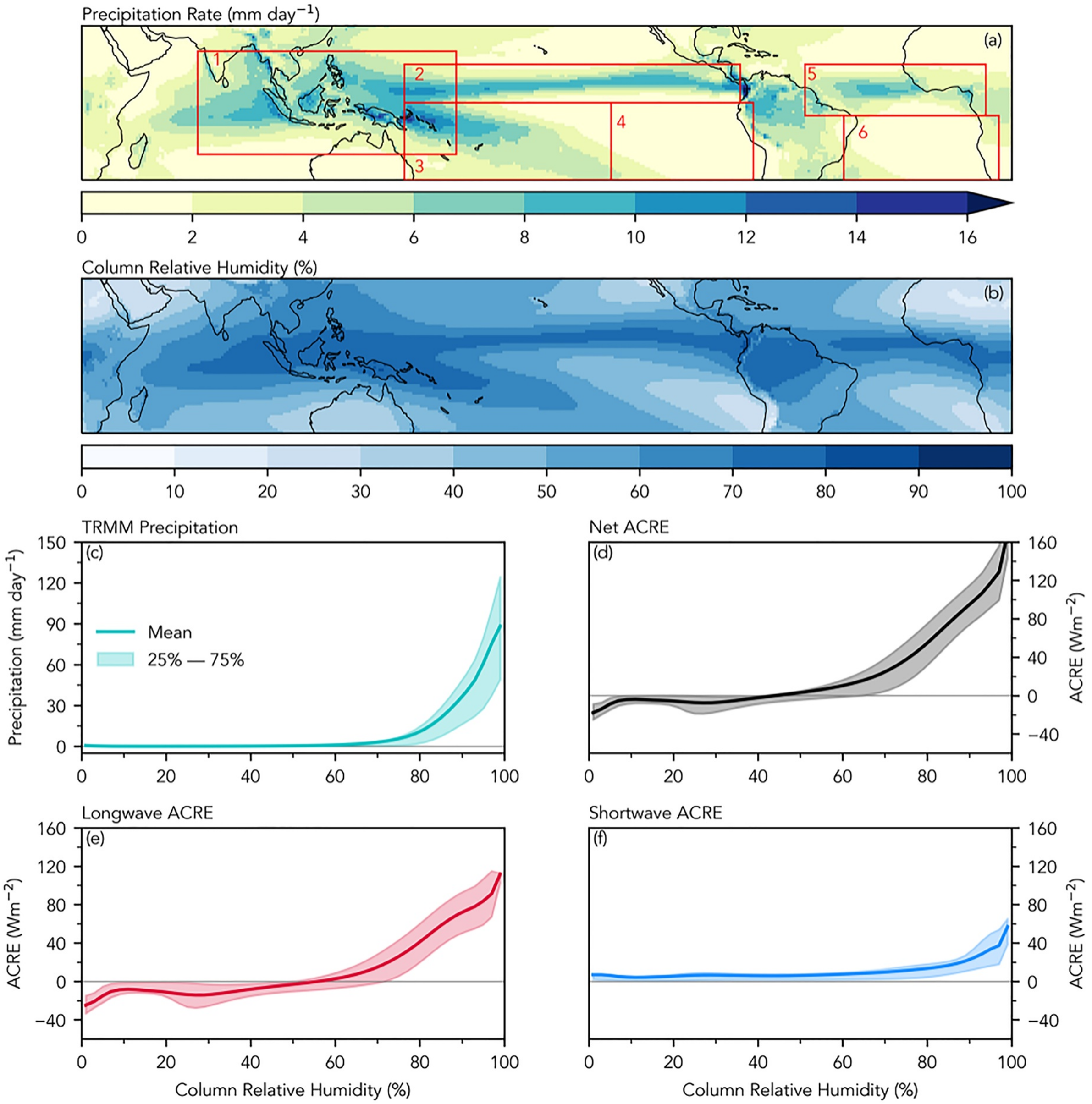

Figure 1. (a): Annual mean precipitation rate from 2001 to 2019, calculated using the TRMM 3b42 product (Huffman et al., 2016). Red boxes 1–6 show the boundaries of six regions used in Section 4.2, with specific boundaries recorded in Table S1. (b): Annual mean column relative humidity calculated from ERA5 reanalysis. (c) TRMM precipitation rate binned by column relative humidity (CRH) for the belt ranging from 30°S to 30°N. The shaded area shows the interquartile range for each CRH bin. (d): Same as (c), but for the atmospheric cloud radiative effect (ACRE). (e) and (f): ACRE from (d), decomposed into longwave and shortwave components.

interquartile range was also found as a measure of the spread of precipitation in each bin. This procedure was repeated for the net, longwave, and shortwave ACRE over the entire tropical belt with results shown in Figure 1c through Figure 1f.

The net ACRE (Figure 1d) is negative or zero when the CRH is small, due to longwave and shortwave contributions which mostly offset (Figures 1e and 1f). When the CRH becomes large the longwave component changes sign and begins to increase. The shortwave component also increases, but at a slower rate. The combination of both terms leads to a rapid increase of the net ACRE above a value of about 70% CRH. This behavior is evocative of the dependence of precipitation on CRH (Figure 1c). As proposed in Section 5, this

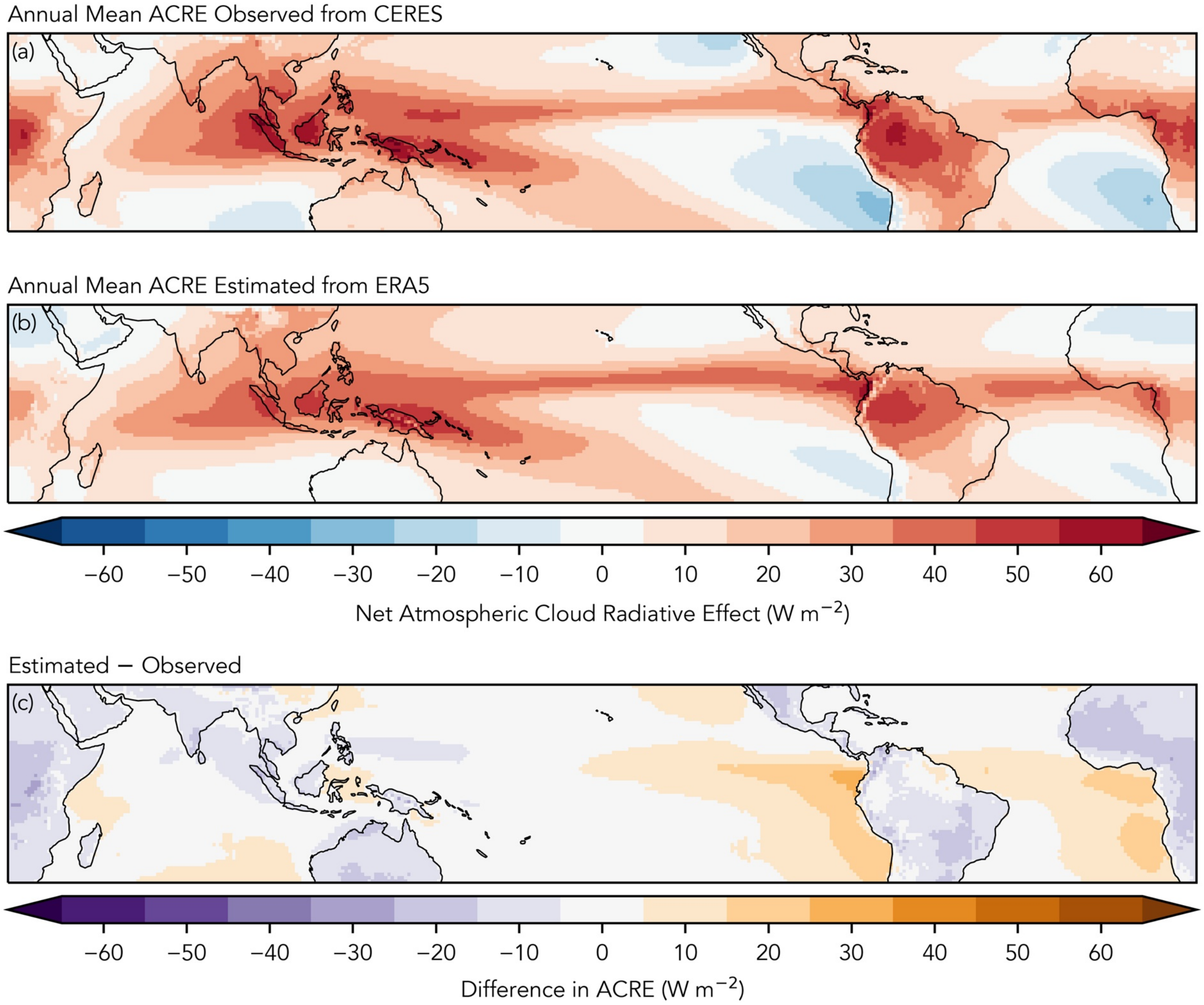

Figure 2. (a): Annual mean ACRE calculated from CERES radiative fluxes. (b): Same as (a), but estimated using CRH calculated from ERA5. (c): Difference calculated as panel (b) minus panel (a).

similarity may be the result of cloud-longwave feedbacks in humid regions of the tropics that promote a shift from convective to stratiform precipitation.

A comparison of Figures 1e and 1f shows that the ACRE is largely determined by the longwave component, consistent with previous studies (Allan, 2011; Slingo & Slingo, 1988). Similar curves result when this analysis is repeated for the six regions shown in Figure 1a even though the regions have markedly different distributions of CRH (Figures S1 and S2 of supporting information). The only obvious difference is due to the influence of marine stratus clouds in the cold tongue regions (Klein & Hartmann, 1993; Schneider et al., 2019; Voigt et al., 2021), which have a large shortwave ACRE and tend to be found in regions with low CRH.

4. Estimating ACRE From CRH

The interquartile range in Figure 1d is small, which indicates little spread in the distribution of the ACRE at a given CRH. This suggests a tight relationship between CRH and ACRE. In this section, we investigate whether the CRH can be used to estimate ACRE, similar to how it has been used to estimate precipitation. To estimate ACRE, the daily mean CRH at a grid cell at a particular timestep was mapped onto the mean curves in Figures 1e and 1f to calculate the longwave and shortwave contributions. These fields were then combined to estimate the net ACRE at each grid cell.

4.1. Time Mean Estimation of ACRE

Figure 2a shows the annual mean ACRE calculated from the observed CERES fluxes. The ACRE is positive over the Indo-Pacific, SPCZ, and ITCZ regions due to the absorption of longwave radiation by convective clouds and organized systems. In the cold-tongue regions, the reflection of sunlight by marine stratus clouds reduces the shortwave radiation that would have otherwise been absorbed, which leads to a negative ACRE. The cooling albedo effect is smaller than the warming greenhouse effect so that the ACRE averaged over the 30°S to 30°N belt is 15.193 W m^{-2}. In Figure 2b the time mean of the estimated ACRE is shown. The estimated ACRE largely reproduces the same spatial structure as the observed ACRE, which includes large positive values over the Indo-Pacific, SPCZ, and ITCZ regions, and negative values in the marine stratus regions. The annual mean ACRE estimated from CRH is 15.203 W m^{-2}; a difference of about 0.01 W m^{-2}.

The difference between the estimated and observed ACRE is shown in Figure 2c. The estimation method has a positive bias in the east Pacific relative to the west Pacific. This is partially due to the longwave CRE at the top of the atmosphere (not shown) and is consistent with Kubar et al. (2007) who found that the temperature of high tropical clouds in the east Pacific was about 5 K warmer compared to similar clouds in the west Pacific. In addition, the estimation method gives negative errors over land compared to mostly positive errors over oceans. We emphasize that this is merely the first attempt to estimate the ACRE from CRH and a more optimal method likely exists, perhaps one that includes the cloud ice path to separate low and high clouds.

4.2. Accuracy of the Estimation on Shorter Time Scales

Figure 3 compares the time series of the observed and estimated monthly mean ACRE anomaly for each of the six regions outlined in Figure 1a. Anomalies were calculated as the monthly average ACRE over the region minus the time mean ACRE for that region for each month, which effectively removes the seasonal cycle. The agreement between the observed and estimated ACRE was evaluated using Pearson's R^2 correlation, which is shown in the lower left-hand corner of each panel.

The Indo-Pacific, SPCZ, and both ITCZ regions each show a high degree of correlation, with R^2 greater than 0.6 or 0.7. The estimation method is able to account for the large peaks in magnitude in the warm pool and pacific ITCZ regions in 2010 and 2015-2016 which are likely associated with the strong El Niño events of those years (National Weather Service, 2020, see Figure S3 through Figure S6 from supporting information). The correlation is slightly lower for the cold tongue regions, with R^2 equal to 0.56 and 0.515 in the Pacific and Atlantic, respectively. Together, this indicates that more than 50% of the variance of the ACRE on monthly time scales is due to variations in CRH for each of these regions (Bony et al., 2004).

The R^2 correlations for the monthly mean time series are recorded in Table S1, alongside the R^2 correlations for the daily mean time series, which were constructed similarly. On daily time scales the agreement is lower than monthly time scales, although the correlation is still greater than 0.6 in the warm pool, and greater than 0.4 in all regions except for the Pacific cold tongue. From this, it appears that the CRH method shows some skill at estimating the ACRE even on time scales shorter than a month.

5. Discussion and Conclusions

We have shown that the ACRE estimated from $1° \times 1°$ daily mean satellite observations varies with the CRH in a way that is similar to the well-documented relationship between precipitation and CRH. Both are small when the CRH is small, and begin to increase rapidly when the CRH exceeds a value near 70%. In addition, we have shown that the CRH can be used to estimate the ACRE similar to how it has been used to estimate precipitation.

Why do ACRE and precipitation behave so similarly when analyzed using the CRH? We believe that this is more than just a coincidence and that the dependence of precipitation on CRH is linked to the ACRE through cloud-longwave feedbacks which have been recently discussed in reference to organized tropical systems.

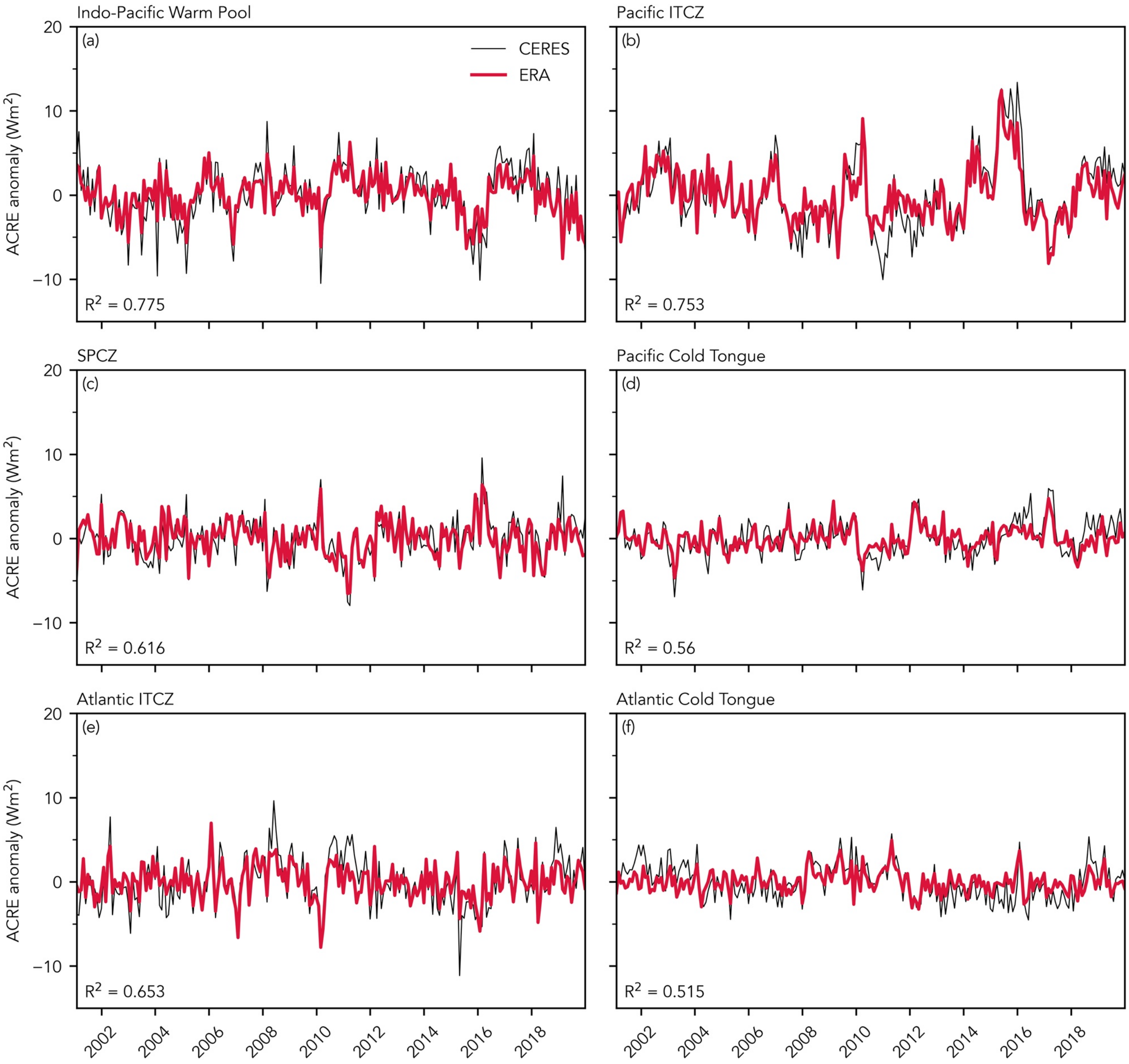

Figure 3. (a) De-seasonalized time series of monthly mean atmospheric cloud radiative effect (ACRE) anomaly averaged over the Indo-Pacific warm pool. The black line shows the ACRE anomaly observed from CERES satellite fluxes, while the red line shows the ACRE anomaly estimated from ERA5. (b)–(f): same as (a), but averaged over, respectively, the Pacific Intertropical Convergence Zone (ITCZ), the south Pacific convergence zone, the Pacific cold tongue, the Atlantic ITCZ, and the Atlantic cold tongue. Outlines of the six regions are shown as boxes in Figure 1 each correlation coefficient used to calculate R^2 is significant at the 0.05 level.

Complementary to this study, Needham and Randall (2021) discuss this type of feedback in the context of a set of idealized simulations. They found that ACRE in extremely humid regions is powerful enough to change the sign of the net radiation tendency, which leads to a convergence of energy into the atmosphere. The net heating drives stratiform ascent which lifts water vapor and moistens the troposphere (Ahmed & Schumacher, 2015; Chikira, 2014; Jenney et al., 2020). In addition, they found that ACRE is independent of SST at a particular CRH in the idealized simulations, consistent with the results presented here. They also performed a set of simulations in which the radiative heating rate is homogenized over the domain. In this case, the CRH distribution is narrower and the extreme precipitation is less frequent, as shown in Figure 4. The homogenized radiation also leads to a reduction in the dry static energy export out of humid regions.

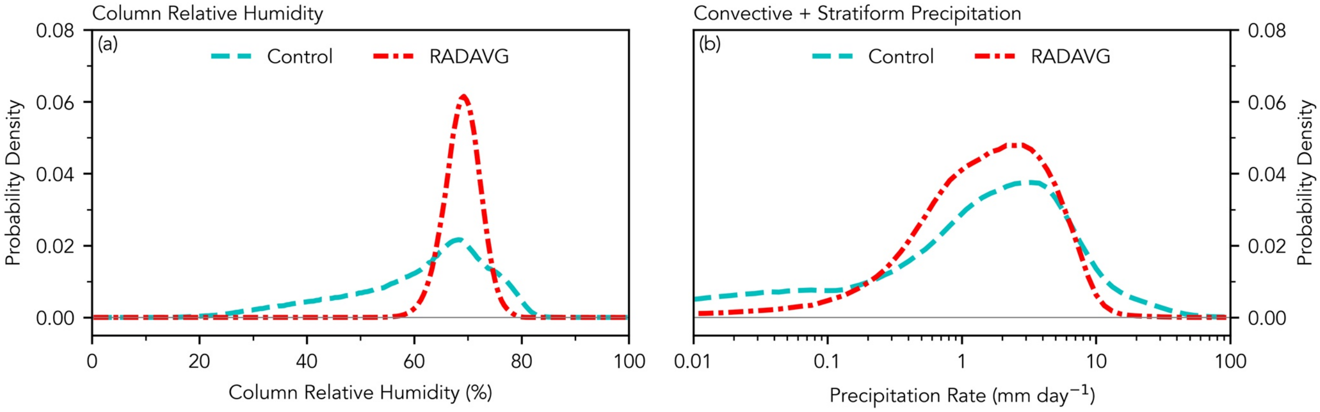

Figure 4. Probability density functions of column radiative humidity (a) and precipitation rate (b) for two simulations analyzed by Needham and Randall (2021). "Control" refers to a simulation performed with a fixed SST of 300 K, no rotation, and uniform insolation. "RADAVG" is identical to Control, except for radiative heating, which is globally averaged at each timestep. Originally from Needham and Randall (2021).

The cloud-longwave feedback described by Needham and Randall (2021) may contribute to the well-documented relationship between precipitation and CRH. Humid regions promote the formation of clouds, which in turn absorb radiation. The ACRE leads to net heating which drives stratiform ascent. This ascent favors a shift from isolated convection to more organized systems that are characterized by stratiform precipitation. As discussed by Ahmed and Schumacher (2015), the area covered by stratiform precipitation increases exponentially at high CRH and appears to be responsible for the characteristic pickup of the precipitation rate above the critical threshold. Future studies should focus on investigating this hypothesis through mechanism-denial experiments which may help to demonstrate causality in the relationship we have shown between ACRE and tropical precipitation.

Data Availability Statement

All of the data used in this study are freely available online. ERA5 reanalysis data were downloaded from the ECMWF Copernicus Climate Data Store (CDS), accessible at https://cds.climate.copernicus.eu/ keyword search "ERA5." CERES SYN1deg_Ed4a data were obtained from the NASA Langley Research Center Atmospheric Science Data Center (ASDC), accessible at https://ceres.larc.nasa.gov/data/ under the heading "Synoptic TOA and surface fluxes and clouds (SYN)." TRMM data were downloaded from the Goddard Earth Sciences Data and Information Services Center (GES DISC), accessible at https://disc.gsfc.nasa.gov/ keyword search "TRMM_3B42."

Acknowledgments

The authors would like to thank two anonymous reviewers for their helpful comments on an earlier version of this manuscript. The authors also thank Professor J. Hurrell and Professor X. Gao for reading M. Needham's M.S. thesis, which includes an earlier version of this study. Support was provided by the National Oceanic and Atmospheric Administration through grant number NA19OAR4590155, and by the National Science Foundation through grant number AGS-1826643, both to Colorado State University.

References

Ahmed, F., & Schumacher, C. (2015). Convective and stratiform components of the precipitation moisture relationship. *Geophysical Research Letters*, *42*(23), 10453–10462. https://doi.org/10.1002/2015gl066957

Albern, N., Voigt, A., Buehler, S. A., & Grützun, V. (2018). Robust and nonrobust impacts of atmospheric cloud-radiative interactions on the tropical circulation and its response to surface warming. *Geophysical Research Letters*, *27*, 4937. https://doi.org/10.1029/2018GL079599

Allan, R. P. (2011). Combining satellite data and models to estimate cloud radiative effect at the surface and in the atmosphere. *Meteorological Applications*, *18*(3), 324–333. https://doi.org/10.1002/met.285

Arnold, N. P., & Randall, D. A. (2015). Global-scale convective aggregation: Implications for the Madden-Julian oscillation. *Journal of Advances in Modeling Earth Systems*, *7*(4), 1499–1518. https://doi.org/10.1002/2015ms000498

Benedict, J. J., Medeiros, B., Clement, A. C., & Olson, J. G. (2020). Investigating the role of cloudradiation interactions in subseasonal tropical disturbances. *Geophysical Research Letters*, *47*(9), e2019GL086817. https://doi.org/10.1029/2019gl086817

Bony, S., Dufresne, J.-L., Le Treut, H., Morcrette, J.-J., & Senior, C. (2004). On dynamic and thermodynamic components of cloud changes. *Climate Dynamics*, *22*(2–3), 71–86. https://doi.org/10.1007/s00382-003-0369-6

Bretherton, C. S., Blossey, P. N., & Khairoutdinov, M. (2005). An energy-balance analysis of deep convective self-aggregation above uniform SST. *Journal of the Atmospheric Sciences*, *62*(12), 4273–4292. https://doi.org/10.1175/JAS3614.1

Bretherton, C. S., Peters, M. E., & Back, L. E. (2004). Relationships between water vapor path and precipitation over the tropical oceans. *Journal of Climate*, *17*(7), 1517–1528. https://doi.org/10.1175/1520-0442(2004)017<1517:rbwvpa>2.0.co;2

Chikira, M. (2014). Eastward-Propagating intraseasonal oscillation represented by Chikira-Sugiyama cumulus parameterization. Part II: Understanding moisture variation under weak temperature gradient balance. *Journal of the Atmospheric Sciences*, *71*(2), 615–639. https://doi.org/10.1175/JAS-D-13-038.1

Dixit, V., Geoffroy, O., & Sherwood, S. C. (2018). Control of ITCZ width by lowlevel radiative heating from upperlevel clouds in aquaplanet simulations. *Geophysical Research Letters*, *45*(11), 5788–5797. https://doi.org/10.1029/2018gl078292

Doelling, D. R., Loeb, N. G., Keyes, D. F., Nordeen, M. L., Morstad, D., Nguyen, C., et al. (2013). Geostationary enhanced temporal interpolation for CERES flux products. *Journal of Atmospheric and Oceanic Technology*, *30*(6), 1072–1090. https://doi.org/10.1175/jtech-d-12-00136.1

Emanuel, K. (2019). Inferences from simple models of slow, convectively coupled processes. *Journal of the Atmospheric Sciences*, *76*(1), 195–208. https://doi.org/10.1175/JAS-D-18-0090.1

Harrop, B. E., & Hartmann, D. L. (2016). The role of cloud radiative heating in determining the location of the ITCZ in aquaplanet simulations. *Journal of Climate*, *29*(8), 2741–2763. https://doi.org/10.1175/JCLI-D-15-0521.1

Hersbach, H., Bell, B., Berrisford, P., Biavati, G., Horányi, A., Muñoz Sabater, J., & Thépaut, J.-N. (2018). *ERA5 hourly data on pressure levels from 1979 to present*. ECMWF. https://doi.org/10.24381/cds.bd0915c6

Hersbach, H., Bell, B., Berrisford, P., Hirahara, S., Horányi, A., Muñoz Sabater, J., et al. (2020). The ERA5 global reanalysis. *Quarterly Journal of the Royal Meteorological Society*, *146*(730), 1999–2049. https://doi.org/10.1002/qj.3803

Huffman, G. J., Bolvin, D. T., Nelkin, E. J., & Adler, R. F. (2016). *TRMM (TMPA) precipitation L3 1 day 0.25 degree × 0.25 degree V7 (TRMM_3B42_Daily)*. Retrieved from https://disc.gsfc.nasa.gov/datasets/TRMM_3B42_Daily_7/summary

Inoue, K., & Back, L. E. (2015). Gross moist stability assessment during TOGA COARE: Various interpretations of gross moist stability. *Journal of the Atmospheric Sciences*, *72*(11), 4148–4166. https://doi.org/10.1175/JAS-D-15-0092.1

Jenney, A. M., Randall, D. A., & Branson, M. D. (2020). Understanding the response of tropical ascent to warming using an energy balance framework. *Journal of Advances in Modeling Earth Systems*, *12*, e2020MS002056. https://doi.org/10.1029/2020MS002056

Khairoutdinov, M. F., & Emanuel, K. (2018). Intraseasonal variability in a cloud-permitting near-global equatorial aquaplanet model. *Journal of the Atmospheric Sciences*, *75*(12), 4337–4355. https://doi.org/10.1175/jas-d-18-0152.1

Klein, S. A., & Hartmann, D. L. (1993). The seasonal cycle of low stratiform clouds. *Journal of Climate*, *6*(8), 1587–1606. https://doi.org/10.1175/1520-0442(1993)006<1587:TSCOLS>2.0.CO;2

Kubar, T. L., Hartmann, D. L., & Wood, R. (2007). Radiative and convective driving of tropical high clouds. *Journal of Climate*, *20*(22), 5510–5526. https://doi.org/10.1175/2007JCLI1628.1

Li, Y., Thompson, D. W. J., & Bony, S. (2015). The influence of atmospheric cloud radiative effects on the large-scale atmospheric circulation. *Journal of Climate*, *28*(18), 7263–7278. https://doi.org/10.1175/jcli-d-14-00825.1

Masunaga, H., & L'Ecuyer, T. S. (2014). A mechanism of tropical convection inferred from observed variability in the moist static energy budget. *Journal of the Atmospheric Sciences*, *71*(10), 3747–3766. https://doi.org/10.1175/JAS-D-14-0015.1

Medeiros, B., Clement, A. C., Benedict, J. J., & Zhang, B. (2021). Investigating the impact of cloud-radiative feedbacks on tropical precipitation extremes. *npj Climate and Atmospheric Science*, *4*(1), 1–10. https://doi.org/10.1038/s41612-021-00174-x

National Weather Service. (2020). *Cold & warm episodes by season*. Retrieved from https://origin.cpc.ncep.noaa.gov/products/analysis_monitoring/ensostuff/ONI_v5.php

Needham, M. R., & Randall, D. A. (2021). *Riehl and Malkus revisited: The role of cloud-radiative effects*. Retrieved from https://www.essoar.org/doi/abs/10.1002/essoar.10506726.1

Popp, M., & Silvers, L. G. (2017). Double and single ITCZs with and without clouds. *Journal of Climate*, *30*(22), 9147–9166. https://doi.org/10.1175/JCLI-D-17-0062.1

Powell, S. W. (2019). Observing possible thermodynamic controls on tropical marine rainfall in moist environments. *Journal of the Atmospheric Sciences*, *76*(12), 3737–3751. https://doi.org/10.1175/jas-d-19-0144.1

Ramanathan, V. (1987). The role of earth radiation budget studies in climate and general circulation research. *Journal of Geophysical Research*, *92*(D4), 4075. https://doi.org/10.1029/JD092iD04p04075

Randall, D. A., Harshvardhan, Dazlich, D. A., & Corsetti, T. G. (1989). Interactions among radiation, convection, and large-scale dynamics in a general circulation model. *Journal of Atmospheric Sciences*, *46*(13), 1943–1970. https://doi.org/10.1175/1520-0469(1989)046<1943:IARCAL>2.0.CO;2

Raymond, D. J. (2000). Thermodynamic control of tropical rainfall. *Quarterly Journal of the Royal Meteorological Society*, *126*(564), 889–898. https://doi.org/10.1002/qj.49712656406

Raymond, D. J., Sessions, S. L., Sobel, A. H., & Fuchs, Ž. (2009). The mechanics of gross moist stability. *Journal of Advances in Modeling Earth Systems*, *1*(3), 9. https://doi.org/10.3894/JAMES.2009.1.9

Raymond, D. J., & Zeng, X. (2005). Modeling tropical atmospheric convection in the context of the weak temperature gradient approximation. *Quarterly Journal of Royal Meteorological Society*, *131*(608), 1301–1320. https://doi.org/10.1256/qj.03.97

Ruppert, J. H., Jr, Wing, A. A., Tang, X., & Duran, E. L. (2020). The critical role of cloud–infrared radiation feedback in tropical cyclone development. *Proceedings of the National Academy of Sciences*, *117*(45), 27884–27892. https://doi.org/10.1073/pnas.2013584117

Rushley, S. S., Kim, D., Bretherton, C. S., & Ahn, M.-S. (2018). Re-examining the non-linear moisture-precipitation relationship over the tropical oceans. *Geophysical Research Letters*, *45*(2), 1133–1140. https://doi.org/10.1002/2017GL076296

Schneider, T., Kaul, C. M., & Pressel, K. G. (2019). Possible climate transitions from breakup of stratocumulus decks under greenhouse warming. *Nature Geoscience*, *12*(3), 163–167. https://doi.org/10.1038/s41561-019-0310-1

Sherwood, S. C., Ramanathan, V., Barnett, T. P., Tyree, M. K., & Roeckner, E. (1994). Response of an atmospheric general circulation model to radiative forcing of tropical clouds. *Journal of Geophysical Research*, *99*(D10), 20829. https://doi.org/10.1029/94jd01632

Slingo, A., & Slingo, J. M. (1988). The response of a general circulation model to cloud longwave radiative forcing. I: Introduction and initial experiments. *Quarterly Journal of Royal Meteorological Society*, *114*(482), 1027–1062. https://doi.org/10.1002/qj.49711448209

Stevens, B., Bony, S., & Webb, M. (2012). *Clouds On-Off Klimate Intercomparison Experiment (COOKIE)*. Retrieved from https://citeseerx.ist.psu.edu/viewdoc/summary?doi=10.1.1.411.3676

Voigt, A., & Albern, N. (2019). No cookie for climate change. *Geophysical Research Letters*, *46*(24), 14751–14761. https://doi.org/10.1029/2019gl084987

Voigt, A., Albern, N., Ceppi, P., Grise, K., Li, Y., & Medeiros, B. (2021). Clouds, radiation, and atmospheric circulation in the present-day climate and under climate change. *Wiley Interdisciplinary Reviews: Climate Change*, *12*(2), e694. https://doi.org/10.1002/wcc.694

Wing, A. A., Emanuel, K., Holloway, C. E., & Muller, C. (2017). Convective self-Aggregation in numerical simulations: A review. *Surveys in Geophysics*, *38*(6), 1173–1197. https://doi.org/10.1007/s10712-017-9408-4

Wolding, B., Dias, J., Kiladis, G., Ahmed, F., Powell, S. W., Maloney, E., & Branson, M. (2020). Interactions between moisture and tropical convection. Part I: The coevolution of moisture and convection. *Journal of the Atmospheric Sciences*, *77*(5), 1783–1799. https://doi.org/10.1175/jas-d-19-0225.1

Wolding, B., Maloney, E. D., & Branson, M. (2016). Vertically resolved weak temperature gradient analysis of the Madden-Julian oscillation in SPCESM. *Journal of Advances in Modeling Earth Systems*, *8*(4), 1586–1619. https://doi.org/10.1002/2016ms000724

Yoneyama, K., Zhang, C., & Long, C. N. (2013). Tracking pulses of the Madden-Julian oscillation. *Bulletin of the American Meteorological Society*, *94*(12), 1871–1891. https://doi.org/10.1175/bams-d-12-00157.1

Zeng, X. (1999). The relationship among precipitation, cloud-top temperature, and precipitable water over the tropics. *Journal of Climate*, *12*(8), 2503–2514. https://doi.org/10.1175/1520-0442(1999)012⟨2503:TRAPCT⟩2.0.CO;2